Oncogene (2015) **34,** 1822–1830

www.nature.com/onc

ORIGINAL ARTICLE

Inhibition of intestinal tumor formation by deletion of the DNA methyltransferase 3a

B Weis[1], J Schmidt[1], H Maamar[2], A Raj[2], H Lin[3], C Tóth[4,5], K Riedmann[1], G Raddatz[1], H-K Seitz[6], AD Ho[7], F Lyko[1] and HG Linhart[6,7,1]

Aberrant *de novo* methylation of DNA is considered an important mediator of tumorigenesis. To investigate the role of *de novo* DNA methyltransferase 3a (Dnmt3a) in intestinal tumor development, we analyzed the expression of Dnmt3a in murine colon crypts, murine colon adenomas and human colorectal cancer using RNA fluorescence *in situ* hybridization (FISH), quantitative PCR and immunostaining. Following conditional deletion of *Dnmt3a* in the colon of APC$^{(Min/+)}$ mice, we analyzed tumor numbers, genotype of macroadenomas and laser dissected microadenomas, global and regional DNA methylation and gene expression. Our results showed increased Dnmt3a expression in colon adenomas of APC$^{(Min/+)}$ mice and human colorectal cancer samples when compared with control tissue. Interestingly, in tumor tissue, RNA FISH analysis showed highest Dnmt3a expression in Lgr5-positive stem/progenitor cells. Deletion of *Dnmt3a* in APC$^{(Min/+)}$ mice reduced colon tumor numbers by ~40%. Remaining adenomas and microadenomas almost exclusively contained the non-recombined *Dnmt3a* allele; no tumors composed of the inactivated *Dnmt3a* allele were detected. DNA methylation was reduced at the Oct4, Nanog, Tff2 and Cdkn1c promoters and expression of the tumor-suppressor genes *Tff2* and *Cdkn1c* was increased. In conclusion, our results show that Dnmt3a is predominantly expressed in the stem/progenitor cell compartment of tumors and that deletion of *Dnmt3a* inhibits the earliest stages of intestinal tumor development.

Oncogene (2015) **34,** 1822–1830; doi:10.1038/onc.2014.114; published online 19 May 2014

INTRODUCTION

DNA methylation at cytosine bases in the context of CpG dinucleotides is required for cell differentiation and phenotypic maintenance of mammalian cells but also has an important role in pathological processes such as tumorigenesis. Multiple studies have shown that DNA methylation in cancer cells is markedly different from healthy tissue: methylation of repetitive elements and intergenic regions is reduced and aberrant *de novo* methylation is found at promoter-associated CpG islands. These alterations can contribute to genetic instability as well as aberrant gene silencing including inactivation of tumor-suppressor genes.[1] The mechanisms that induce such aberrant DNA methylation, however, are not fully understood. Two enzymes are considered to catalyse *de novo* methylation in mammalian cells: the DNA methyltransferases 3a (Dnmt3a) and 3b (Dnmt3b).[2,3] Both of these Dnmts are required for development, as they are expressed at high levels during early embryogenesis and deletion of these enzymes is embryonic or perinatal lethal.[2]

Dnmt3a and Dnmt3b have been implicated as possible mediators of tumor-associated *de novo* methylation, however, the role of Dnmt3a in the context of tumorigenesis has not been fully clarified: transgenic expression of Dnmt3a was shown to promote intestinal tumor development in one study,[4] suggesting an oncogenic role of Dnmt3a, whereas another study failed to confirm such an effect.[5] In contrast, Dnmt3a mutations are frequently found in acute myeloid leukemia and correlate with an adverse outcome in this disease,[6] suggesting a tumor-suppressor role of Dnmt3a. The role of Dnmt3a in the context of intestinal tumorigenesis, therefore, remains unclear and so far has not been addressed by a loss of function experiment.

To further clarify the role of Dnmt3a in the development of intestinal tumors, we characterized Dnmt3a expression in the intestinal mucosa and colon tumors and analyzed the effect of *Dnmt3a* deletion in intestinal epithelial cells on colon tumorigenesis in the APC$^{(Min/+)}$ mouse model. In this study, we show that Dnmt3a is preferentially expressed in Lgr5-positive stem and progenitor cells in normal mucosa and neoplastic tissue. We also show that deletion of *Dnmt3a* results in regional DNA hypomethylation and increased expression of tumor-suppressor genes and inhibits the earliest stages of intestinal tumor formation in APC$^{(Min/+)}$ mice.

RESULTS

Dnmt3a expression in colon mucosa and colon tumors

To analyze Dnmt3a expression in colon epithelial cells and colon tumors of APC$^{(Min/+)}$ mice with single-cell resolution, we conducted RNA fluorescence *in situ* hybridization (FISH) analysis using probes directed against Dnmt3a and the intestinal stem and progenitor cell marker Lgr5. All Dnmt3a-specific probes were positioned within unique regions of the Dnmt3a mRNA to avoid cross-hybridization with other DNA methyltransferases (Supplementary Figure 1). Co-staining with probes directed against Lgr5 mRNA was conducted to facilitate orientation within

[1]Division of Epigenetics (A130), German Cancer Research Center (DKFZ), Heidelberg, Germany; [2]Department of Bioengineering, University of Pennsylvania, Philadelphia, PA, USA; [3]Department of Ophthalmology, Massachusetts Eye and Ear Infirmary, Harvard Medical School, Boston, MA, USA; [4]Department of Pathology, University of Heidelberg, National Center for Tumor Diseases (NCT) Tissue Bank, Heidelberg, Germany; [5]Department of Pathology, Heinrich Heine University, Düsseldorf, Germany; [6]Department of Medicine, Salem Medical Center, Alcohol Research Center, University of Heidelberg, Heidelberg, Germany and [7]Department of Hematology/Oncology, University of Heidelberg Medical Center, Heidelberg, Germany. Correspondence: Dr HG Linhart, Division of Epigenetics (A130), German Cancer Research Center (DKFZ), Im Neuenheimer Feld 280, Heidelberg, Baden-Württemberg 69120, Germany.
E-mail: heinz.linhart@nct-heidelberg.de
Received 22 October 2013; revised 13 March 2014; accepted 26 March 2014; published online 19 May 2014

individual crypts and to allow comparison of Dnmt3a expression in crypt stem and progenitor cells (Lgr5 positive), crypt differentiated cells (Lgr5 negative), tumor stem and progenitor cells (Lgr5 positive) and tumor differentiated cells (Lgr5 negative). To control for staining variability and to allow for quantitative comparison of tumor and mucosa, we only used colon cross-sections that included both tumor tissue and normal mucosa. As illustrated in Figure 1a and Supplementary Figure 2, Dnmt3a expression in normal mucosa was highest in Lgr5-positive crypt stem and progenitor cells and Lgr5-negative cells close to the crypt bottom, whereas expression progressively decreased toward the upper part of the crypt. This expression gradient was also detectable by immunohistochemistry (Figure 1b and Supplementary Figure 3) using a polyclonal antibody directed against the N-terminal region of Dnmt3a, which has no homology to Dnmt1, Dnmt2, Dnmt3b or Dnmt3L. Our data therefore suggest that Dnmt3a is preferentially expressed in intestinal stem cells and undifferentiated progenitor cells of the intestinal mucosa.

Interestingly, in tumor tissue RNA FISH analysis and immunohistochemistry showed increased average expression of Dnmt3a when compared with normal crypts. In analogy to normal crypts, Dnmt3a expression was higher in Lgr5-positive than in Lgr5-negative cells (Figure 1a). RNA FISH analysis also showed individual pockets with expansion of Lgr5-positive tumor stem and progenitor cells within tumor tissue (data not shown).

We next conducted quantitative PCR (qPCR) Dnmt3a expression analysis of 41 human colorectal cancer samples and 41 matched colon mucosa samples. Primers were separated by an intron and were positioned within unique regions of Dnmt3a to avoid cross reactivity with other DNA methyltransferases. As shown in Figure 1c and Supplementary Figure 4, Dnmt3a expression was increased in 23 out of 41 colorectal cancer samples, 10 out

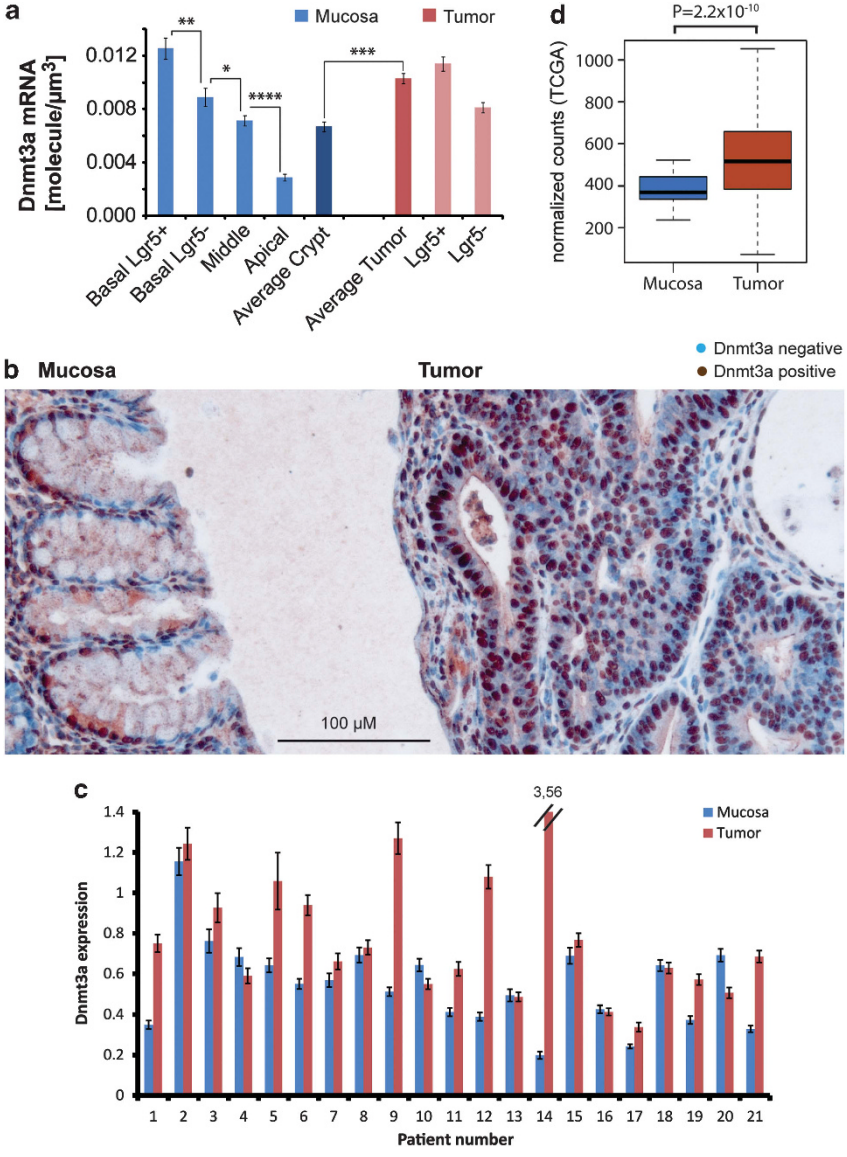

Figure 1. Dnmt3a expression analysis of colon mucosa and colon tumors. (**a**) Quantitative RNA FISH analysis of Dnmt3a and Lgr5 (stem cell marker) expression in transverse colon sections of $APC^{(Min/+)}$ mice containing both normal mucosa and tumor tissue. ****$P = 9e-14$; ***$P = 0.00007$; **$P = 0.003$; *$P = 0.012$; error bars = s.d. (**b**) Immunostaining with Dnmt3a-specific antibody of hematoxylin counter-stained transverse colon sections of $APC^{(Min/+)}$ mice containing both normal mucosa and tumor tissue. (**c**) Quantitative RT–PCR expression analysis of Dnmt3a relative to β-actin of 21 human colorectal cancers and matched mucosa. Error bars = s.d. (**d**) Expression levels of Dnmt3a were analyzed in the TCGA colon cancer RNAseq data set. Box plots show expression levels for control colon mucosa tissue ($n = 41$) and for tumors ($n = 258$).

of 41 sample pairs did not show a difference in expression and 8 out of 41 sample pairs showed increased expression in the mucosa when compared with cancer tissue. Similarly, analysis of Dnmt3a expression levels in 258 colon cancer and 41 control mucosa samples showed a significantly ($P = 2.2 \times 10^{-10}$) increased expression level in tumors (Figure 1d). In agreement with possible expansion of stem cells and undifferentiated cells in tumors, qPCR analysis showed increased Lgr5 expression in cancer samples compared with matched mucosa samples (Supplementary Figure 5).

Deletion of Dnmt3a inhibits tumor formation

To test the role of Dnmt3a in intestinal tumorigenesis, we conducted conditional deletion of *Dnmt3a* in colon epithelial cells of the murine $APC^{(Min/+)}$ tumor model using a conditional *Dnmt3a* allele ($Dnmt3a^{(2lox)}$) with the catalytic domain (exons 17–19) flanked by loxP sites.[7,8] For *Dnmt3a* deletion in intestinal epithelial cells, we used a previously described transgenic strain expressing Cre recombinase under the control of the fatty acid binding protein promoter ($Fabpl^{4xat-132}$-Cre), which is active in epithelial cells of the distal intestinal tract starting at embryonic day 13.5.[9,10]

To allow for comparison of the tumor phenotype in the presence of the functional *Dnmt3a* allele and the inactivated *Dnmt3a* allele, we generated $Dnmt3a^{(2lox/2lox)}$ $APC^{(Min/+)}$ mice that were either positive (Cre^+) or negative (Cre^-) for the $Fabpl^{4xat-132}$-Cre transgene. Assessment of colon tumors and tissue harvesting was conducted at 5 months of age. As shown in Figure 2a, the average colon tumor number in Cre^+ mice was reduced when compared with Cre^- mice, however, the difference only narrowly reached statistical significance. No significant difference was observed when comparing tumor size (Figure 2b).

Residual colon tumors predominantly contain the functional Dnmt3a allele

Previous studies had shown that recombination efficiency of the $Fabpl^{4xat-132}$-Cre transgene in the colon mucosa is incomplete and reaches approximately 50%.[10] We therefore analyzed the genotype of the colon mucosa and colon tumors of Cre^+ mice using a competitive PCR assay that allowed simultaneous detection of the conditional (2lox) allele and the recombined (1lox) allele. Plasmids containing the 1lox- and 2lox-specific PCR products, respectively, were used to generate quantitative references at different molar ratios. Mucosa samples and colon tumors from Cre^- mice were used as controls. As shown in Figure 2c, the relative intensity of the 1lox and 2lox band of each standard closely reflected the expected ratio, indicating that the relative intensity of the PCR bands could be used for semi-quantitative assessment of allelic content. As expected, analysis of mucosa and tumors from Cre^- mice yielded a 2lox band only, because of the absence of the $Fabpl^{4xat-132}$-Cre transgene. In contrast, analysis of Cre^+ colonic mucosa yielded 1lox and 2lox bands of similar intensity, suggesting recombination of approximately 30–50% of the Dnmt3a 2lox alleles, which is in good agreement with previous studies.[10] Interestingly, we found that the majority of tumors from Cre^+ contained the Dnmt3a 2lox allele only. Only a few Cre^+ tumors showed a weak 1lox-specific band, and in most of these cases, the relative 1lox content was estimated at less than 10% (Figure 2c, Supplementary Table 1). This strongly suggests that colon tumors in Cre^+ mice almost exclusively originated from Dnmt3a 2lox cells and not from Dnmt3a 1lox-containing cells. To confirm this finding and to further quantify the 1lox content of Cre^+ tumors, we developed a probe-based qPCR assay to measure 1lox/2lox allele ratios.[11] As shown in Supplementary Table 2, individual data of probe-based qPCR analysis of 1lox/2lox allele ratios correlated well with the corresponding data of the competitive PCR analysis. Thus, both methods demonstrated negative selection of the recombined 1lox allele in tumor tissue when compared with normal mucosa tissue of Cre^+ mice.

Microadenomas contain the functional Dnmt3a allele

To determine whether Dnmt3a deletion also affected development of tumor precursor lesions, we conducted 1lox/2lox allele genotyping of 10 colonic microadenomas in Cre^+ mice. Microadenomas can be identified by morphology, size and increased nuclear β-catenin staining.[12] For this we generated serial horizontal sections of flattened colon samples: for each sample, one mucosa section was submitted to β-catenin immunostaining to allow for microadenoma identification and at least three neighboring sections were used for microadenoma harvesting using laser microdissection (Figure 3a). For 1lox/2lox allele genotyping, each microadenoma sample was subjected to three separate nested PCR reactions: 1lox reaction, 2lox reaction and reference PCR reaction. Placement of primers is illustrated in Figure 3b, morphologically normal Cre^+ and Cre^- mucosa was used as control tissue. As expected, 2lox allele only was detected in Cre^- mucosa, whereas analysis of Cre^+ mucosa revealed 1lox and 2lox bands of approximately equivalent intensity. In contrast to normal Cre^+ mucosa, genotyping of microadenomas in Cre^+ mice showed presence of the 2lox allele only, suggesting negative selection of the 1lox allele in these tumor precursor lesions (Figure 3c).

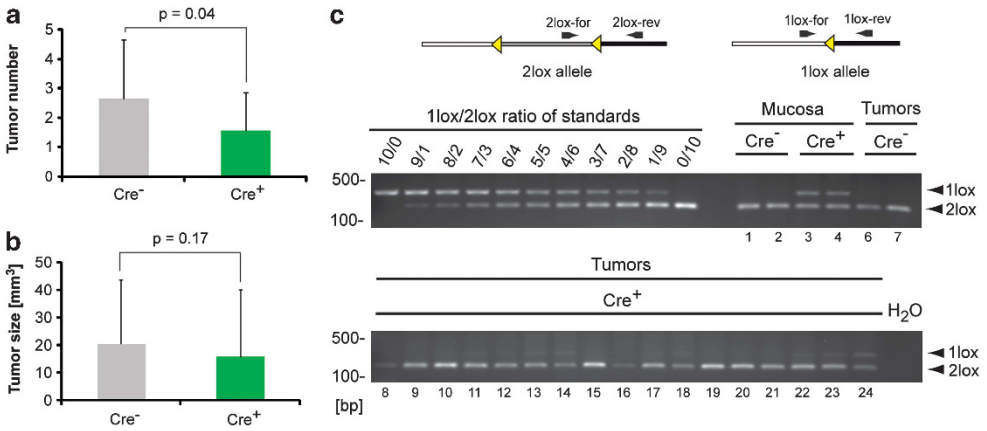

Figure 2. Decreased formation of colon adenomas in mice with Fabp-Cre-mediated deletion of Dnmt3a. (**a**) Mean colon tumor numbers of Cre^+ and Cre^- mice ($n(Cre^+) = 63$; $n(Cre^-) = 65$). (**b**) Mean size of colon tumors (40 Cre^+ tumors, 24 Cre^- tumors), error bars = s.d. (**c**) Illustration of competitive PCR analysis and results of 1lox/2lox genotyping of tumors and mucosa tissue. Yellow triangles = loxP sites.

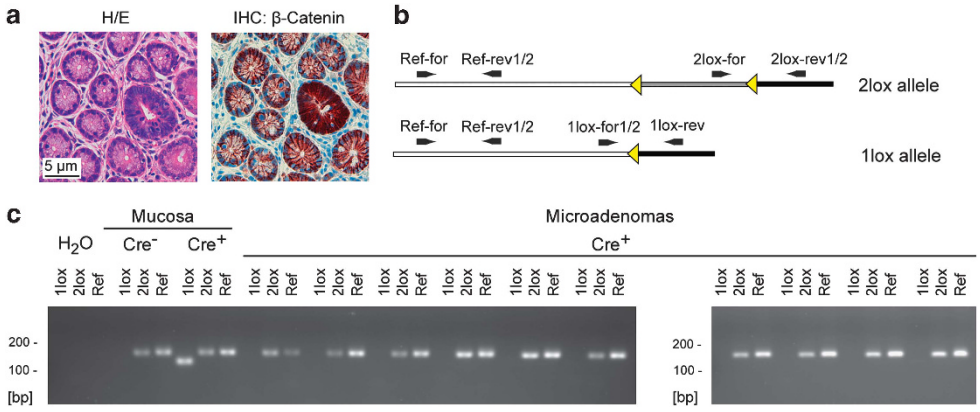

Figure 3. Microadenomas of Cre$^+$ mice contain the 2lox allele only. (**a**) Representative flat colon mucosa section of an APC$^{(Min/+)}$ mouse showing a microadenoma visualized by H/E and β-catenin immunostaining (IHC). (**b**) Illustration of nested PCR analysis used for 1lox/2lox genotyping of microadenomas. (**c**) 1lox/2lox genotyping of 10 laser microdissected microadenomas harvested from different Cre$^+$ mice. 1lox = 1lox allele, 2lox = 2lox allele, ref = reference region upstream of the loxP sites, yellow triangles = loxP sites.

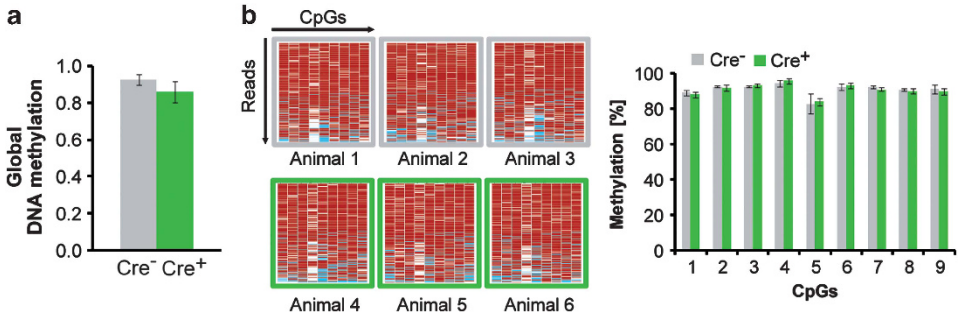

Figure 4. Analysis of global DNA methylation in mice with Fabp-Cre-mediated deletion of Dnmt3a. (**a**) Luminometric Methylation Assay analysis of colon mucosa samples from 3 Cre$^+$ and 2 Cre$^-$ mice. Error bars = s.d. Mean Cre$^+$ = 0.92/s.d. = 0.03; mean Cre$^-$ = 0.86/s.d. = 0.06. (**b**) 454 bisulfite sequencing analysis of the Line1 element of Cre$^+$ and Cre$^-$ colon mucosa samples ($n = 3$ each). Left section = heat maps (red = methylated cytosine, blue = unmethylated cytosine, read number per sample (1/2/3/4/5/6): 244/231/228/236/203/233); right section = quantitative analysis (error bars = s.d).

Dnmt3a deletion causes regional loss of DNA methylation

To determine whether Dnmt3a deletion affected global DNA methylation, we conducted Luminometric Methylation Assay analysis of DNA derived from colon mucosa of Cre$^+$ and Cre$^-$ mice. As shown in Figure 4a, a minor reduction of global DNA methylation was detected in Cre$^+$ tissue when compared with Cre$^-$ tissue. As cytosine methylation of the repetitive LINE1 element is frequently used as a surrogate marker for global DNA methylation,[13] we also conducted bisulfite sequencing analysis of the LINE1 element. As shown in Figure 4b, no difference in LINE1 element methylation was detected when comparing Cre$^+$ and Cre$^-$ mucosa, suggesting that Dnmt3a deletion caused minor to no changes in global DNA methylation.

Previous studies had shown that Dnmt3a is involved in the establishment of genomic imprints as well as *de novo* methylation of the pluripotency genes *Oct4* and *Nanog* during embryonic development.[14,15] We therefore conducted bisulfite sequencing analysis of the Oct4 and Nanog promoter regions and the imprinted locus H19 DMR. As shown in Figures 5b and c, a subset of CpG positions within the H19 DMR and Nanog promoter showed reduced cytosine methylation in Cre$^+$ colon mucosa when compared with Cre$^-$ mucosa. In addition, a significant methylation decrease of the entire Oct4 promoter region was observed in the colon mucosa of Cre$^+$ mice (Figure 5a): Cre$^+$ tissue contained approximately 40% demethylated Oct4 promoter sequences, which correlated with the previously determined Dnmt3a deletion efficiency of 30–50% (Figure 2c and Supplementary Table 2).

Deletion of Dnmt3a causes promoter demethylation and increased expression of tumor-suppressor genes

To investigate possible molecular causes of the tumor phenotype, we conducted microarray-based expression analysis of 42 281 annotated murine transcripts using three Cre$^+$ and three Cre$^-$ colon mucosa samples. In all, 334 transcripts were significantly increased (⩾1.5-fold; $P < 0.05$) and 382 transcripts were significantly reduced (⩾1.5 fold reduction; $P < 0.05$) in Cre$^+$ samples when compared with Cre$^-$ samples (Supplementary Figure 6a). The majority of differentially expressed genes was associated with cell growth, cell proliferation, cell death and cell survival (Supplementary Figure 6b). No significant change in gene expression was observed for the previously analyzed loci Oct4, Nanog and Igf2, which is regulated by the H19 DMR (Supplementary Figure 6c). Also, qPCR analysis failed to show significant expression changes of the *Oct4* gene (Figure 6a).

Among transcripts with increased expression in Cre$^+$ mucosa we identified Tff2 (8.2-fold increase) and Cdkn1c (2-old increase) as putative tumor-suppressor genes[16–19] (Supplementary Figure 6c). In agreement with the microarray analysis, increased expression of both Tff2 and Cdkn1c in Cre$^+$ mucosa was confirmed by qPCR analysis (Figures 6b and c). We next tested whether these

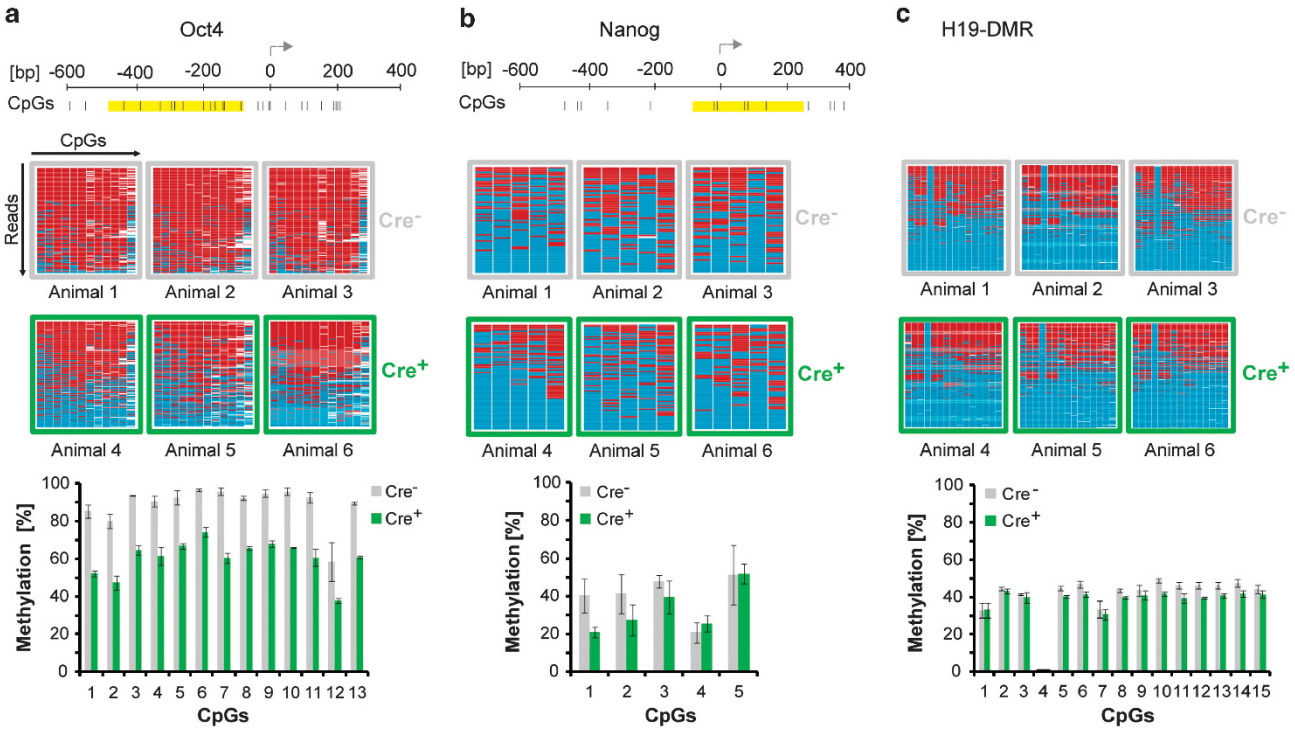

Figure 5. 454 bisulfite sequencing analysis of putative Dnmt3a target regions in mice with Fabp-Cre-mediated deletion of Dnmt3a in colon mucosa ($n = 3$ each). Top section = map of analyzed region (yellow = analyzed region, arrow = transcriptional start site); middle section = heat maps (red = methylated cytosine, blue = unmethylated cytosine); bottom section = quantitative analysis (error bars = s.d.). (**a**) Oct4 promoter region (read number per sample (1/2/3/4/5/6): 164/198/195/183/173/169); (**b**) Nanog promoter region (read number per sample (1/2/3/4/5/6): 67/55/62/83/83/59); (**c**) H19 DMR (read number per sample (1/2/3/4/5/6): 207/225/257/225/229/271).

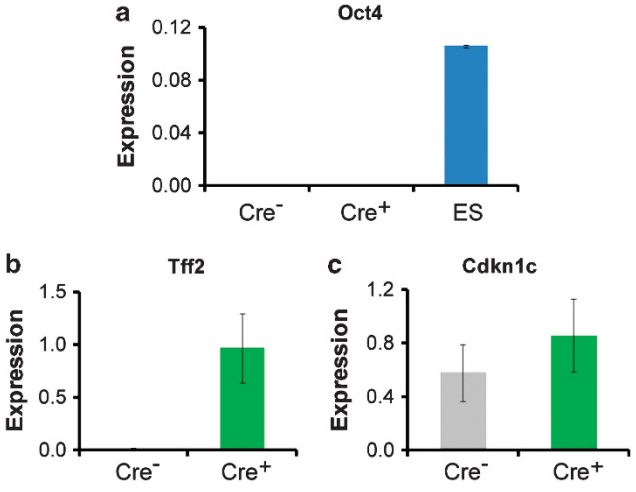

Figure 6. Quantitative RT-PCR expression analysis of (**a**) Oct4; (**b**) Tff2; (**c**) Cdkn1c in mice with Fabp-Cre-mediated deletion of Dnmt3a in colon mucosa ($n = 3$ each). Reference = Gapdh, error bars = s.d., ES, murine embryonic stem cells.

expression changes were associated with altered promoter methylation. In the case of Tff2, we analyzed cytosine methylation of eight CpG positions covering the transcriptional start site (bp −222 to +140). As shown in Figure 7a, Cre$^+$ mucosa showed reduced cytosine methylation resulting in increased appearance of unmethylated *Tff2* alleles. The largest methylation decrease was measured at CpGs 5 (relative reduction 71%), 7 (relative reduction 28%) and 8 (relative reduction 22%).

As expected for an imprinted locus, bisulfite sequencing analysis of the Cdkn1c promoter (48 CpGs from −467 to −54) in control mucosa (Cre$^-$) showed similar proportions of mostly methylated and mostly unmethylated sequences. Methylated sequences showed a distinctive pocket of reduced methylation at positions 22–24 with CpG 22 showing an overall methylation rate of 17% only (Figure 7b). Analysis of Cre$^+$ mucosa did not show changes in methylation at CpG positions 1–19, however, reduced cytosine methylation was detected in the second half of the analyzed Cdkn1c sequence with the most significant reduction observed at CpG position 22 (42% relative methylation decrease). Interestingly, CpG position 22 lies in the middle of the sequence 5′-CCCCGCCCCC-3′, which corresponds to the consensus binding motif of the Sp1 transcription factor (http://jaspar.genereg.net/) and previous studies have confirmed binding of Sp1 to this position of the Cdkn1c promoter.[20]

Finally, we also used bioinformatical analysis to determine whether gene deregulation in our model can further be linked to Dnmt3a target regions. It has been reported that conserved domains of reduced DNA methylation—also referred to as DNA methylation canyons—are targeted by Dnmt3a.[21] We therefore used published data for the mouse colon methylome[22] to determine whether transcriptional deregulation of canyons was observed in the mucosa of Cre+ mice. Our previous gene expression analysis had shown aberrant expression of 1.7% of all transcripts analyzed in the colon mucosa of Cre$^+$ mice. Subsequent bioinformatic analysis showed that 3.3% (36/1106) of all canyons in Cre$^+$ mucosa were associated with transcriptional deregulation, indicating a twofold enrichment of aberrant gene expression in putative Dnmt3a target regions (Supplementary Table 3). This finding further supports the concept that transcriptional deregulation in Cre$^+$ mucosa is at least partially a direct consequence of Dnmt3a deletion.

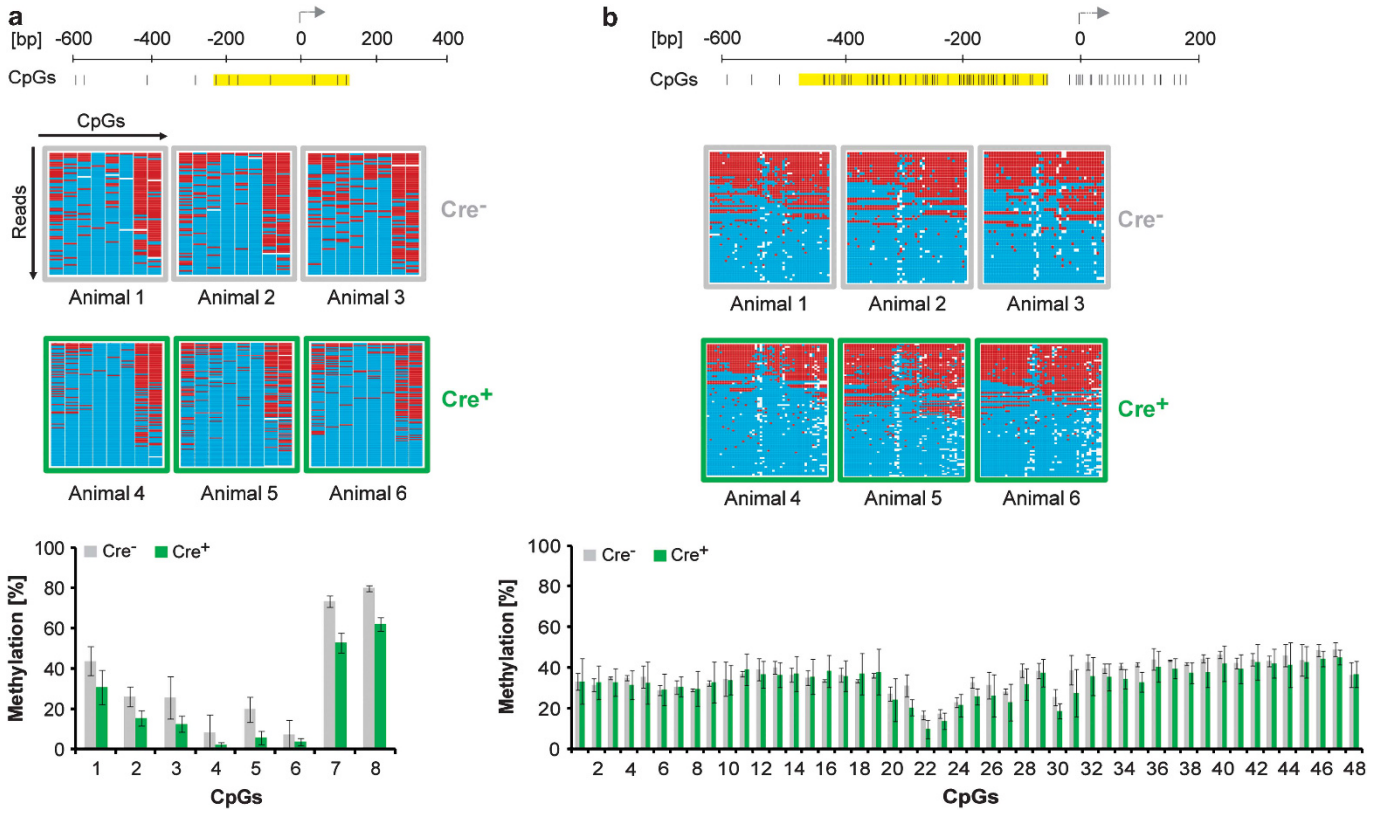

Figure 7. 454 bisulfite sequencing analysis of the Tff2 and Cdkn1c promoter regions in mice with Fabp-Cre-mediated deletion of Dnmt3a in colon mucosa ($n = 3$ each). Map of analyzed region (yellow = analyzed region, arrow = transcriptional start site); heat maps (red = methylated cytosine, blue = unmethylated cytosine); quantitative analysis (error bars = s.d.). (**a**) Tff2 (read number per sample (1/2/3/4/5/6): 69/78/64/101/133/118); (**b**) Cdkn1c (read number per sample (1/2/3/4/5/6): 64/52/42/72/91/70).

DISCUSSION

Aberrant *de novo* methylation of CpG islands has been reported for almost every type of human cancer and many studies suggest that such tumor-associated *de novo* methylation is causally involved in the neoplastic process.[23] Dnmt3a and Dnmt3b are considered the major *de novo* methyltransferases of mammalian cells and therefore have been implicated as possible mediators of aberrant *de novo* methylation in cancer.[4,5]

To characterize the role of Dnmt3a in intestinal tumorigenesis, we first analyzed Dnmt3a expression in normal colon crypts and colon adenomas of APC$^{(Min/+)}$ mice and human colorectal carcinoma samples. Our analyses showed that Dnmt3a expression was significantly increased in colon adenomas of APC$^{(Min/+)}$ mice and in human colorectal cancer samples. These findings are consistent with published data that had shown increased expression of Dnmt3a in multiple human cancer types, such as lung cancer,[24] pancreatic cancer,[25] ovarian cancer,[26] cervix cancer,[27] neuroendocrine tumors,[28] retinoblastoma[29] and colon cancer.[4] In addition, our results indicate that Dnmt3a is predominantly expressed in the intestinal stem and progenitor cell compartment of normal mucosa and tumor tissue. Also, colon adenomas showed distinctive aggregates of Lgr5-positive tumor cells. These findings support the concept that increased Dnmt3a expression in tumors possibly reflects expansion of tumor stem and progenitor cells, rather than cell autonomous deregulation of Dnmt3a gene expression. Indeed, our analyses showed increased expression of the stem cell marker Lgr5 in human colorectal cancer tissue, suggesting expansion of the stem/progenitor cell compartment in these tumors.

To further test the role of Dnmt3a in intestinal tumorigenesis, we conducted Cre/Lox-mediated deletion of *Dnmt3a* in colon epithelial cells of the APC$^{(Min/+)}$ mouse model. Consistent with previous studies using the Fabp-Cre transgene that had reported a mosaic pattern of gene deletion in the intestinal mucosa,[10] we observed incomplete deletion of *Dnmt3a* in the colon mucosa resulting in 30–50% inactivated (1lox) allele and 70–50% active (2lox) *Dnmt3a* allele in colon epithelial cells of Fabp-Cre^{+} mice. When comparing Cre^{+} and Cre^{-} mice, we observed a moderate reduction (approximately 40%) of colon tumor numbers as a consequence of partial *Dnmt3a* deletion with no difference in tumor size. Because of tumor number variability, the difference in tumor numbers between Cre^{+} and Cre^{-} mice only narrowly reached statistical significance. Importantly, however, colon adenomas of Cre^{+} mice predominantly contained the active (2lox) *Dnmt3a* allele. No tumors composed of the inactive (1lox) *Dnmt3a* allele were detected. The minor content of 1lox allele in a few tumor samples was most likely caused by the harvesting process with admixture of 1lox-containing normal mucosa in the tumor sample. Microadenomas of Cre^{+} mice also showed the presence of the 2lox allele only, suggesting that Dnmt3a activity is required for the earliest stages of intestinal tumor development. Our finding that Dnmt3a is predominantly expressed in Lgr5-positive tumor stem and progenitor cells supports the hypothesis that tumor inhibition after *Dnmt3a* deletion is possibly caused by impairment of the tumor stem/progenitor cell compartment.

In contrast to our findings, a recent study showed increased tumor progression following *Dnmt3a* deletion in a k-ras-induced lung tumor model,[7] indicating a tumor-suppressor function of Dnmt3a. It is possible that differences in tumor phenotype after *Dnmt3a* inhibition/deletion are attributable to differences in the

tumor model—k-ras oncogene model versus APC tumor-suppressor model—and possibly also differences in tissue type. In analogy, contrasting tumor phenotypes in different tumor models have been observed in the context of *Dnmt3b* deletion: *Dnmt3b* deletion was shown to inhibit intestinal tumor formation in the $APC^{(Min/+)}$ model,[10] whereas myc-induced mouse lymphomagenesis was accelerated by *Dnmt3b* knockout.[30]

Our analyses showed minor to no global DNA methylation decrease as a consequence of partial *Dnmt3a* deletion, however, some changes might have been masked by remaining cells with a functional *Dnmt3a* allele. In agreement with this observation, a recent analysis of lung tumor tissue had shown a moderate decrease of global DNA methylation as a consequence of *Dnmt3a* deletion.[31]

We detected moderate demethylation at the Nanog promoter and approximately 40% DNA methylation decrease at the Oct4 promoter that correlated well with the 30–50% Dnmt3a recombination efficacy of our model. As the Fabp Cre transgene is actively starting at embryonic day 13.5, such regional loss of methylation could be caused by the loss of Dnmt3a-mediated *de novo* methylation and/or loss of Dnmt3a-mediated maintenance methylation. A previous study had shown that Dnmt3a is required for *de novo* methylation of *Oct4* and *Nanog* during early phases of embryonic stem cell differentiation.[14] Since the Fabp-Cre transgene is activated after *de novo* methylation of *Oct4* and *Nanog* is completed (embryonic day E13.5), our results demonstrate that Dnmt3a is not only required for *de novo* methylation but also for maintenance methylation of these loci. Interestingly, despite decreased methylation of *Oct4* and *Nanog*, expression of these genes was not altered in Cre^+ mice, possibly due to the presence of additional suppressive epigenetic marks and the absence of appropriate transcription factors in this tissue.

Our RNA expression analyses of Cre^+ mucosa showed enrichment of aberrant gene expression in putative Dnmt3a target regions and deregulation of genes involved in cell growth and proliferation, including upregulation of the tumor-suppressor genes *Tff2* and *Cdkn1c*. Also, promoter methylation of *Tff2* and *Cdkn1c* was decreased in Cre^+ mucosa. Interestingly, in the case of *Cdkn1c*, the largest relative methylation decrease was observed at CpG22, which lies in the center of a consensus binding motif of the Sp1 transcription factor and methylation at CpG22 was shown to inhibit attachment of Sp1 to this site.[20] It is therefore possible that demethylation at CpG22 in the mucosa of Cre^+ mice is particularly relevant with regard to the observed transcriptional upregulation of Cdkn1c.

Human studies had demonstrated *de novo* methylation and downregulation of Tff2 in gastric cancer and deletion of *Tff2* was shown to promote gastric cancer in a murine tumor model.[16,17] Cdkn1c inhibits Cyclin-CDK complexes and thereby causes G1 cell cycle arrest, and previous studies have shown increased methylation and transcriptional downregulation of this gene in tumor tissue.[18] Demethylation and transcriptional upregulation of both tumor-suppressor genes therefore could have contributed to the decreased tumor formation observed in mice with Dnmt3a deletion.

Collectively, our data support the hypothesis that Dnmt3a is preferentially expressed in tumor stem and progenitor cells and that inhibition of Dnmt3a increases expression of tumor-suppressor genes and impairs intestinal tumorigenesis. Our data raise the question whether prophylactic inhibition of Dnmt3a might help prevent intestinal tumor formation, particularly, in high-risk populations such as familial adenomatous polyposis(FAP) patients.

MATERIALS AND METHODS

Mice and human samples

The $Dnmt3a^{(2lox/2lox)}$, $Fabpl^{4xat\text{-}132}\text{-}Cre^{(+/-)}$, $APC^{(Min/+)}$ transgenic mice were generated in analogy to previously described $Dnmt3b^{(2lox/2lox)}$, $Fabpl^{4xat\text{-}132}\text{-}Cre^{(+/-)}$, $APC^{(Min/+)}$ mice.[10] The conditional Dnmt3a allele was generated as outlined in study by Nguyen *et al*.[8] All experimental mice were backcrossed at least six generations into C57BL/6 mice. For analysis, 128 5-month-old mice (63 Cre^+ and 65 Cre^-) were used. All animal experiments in the context of this study were approved by the MIT Department of Comparative Medicine, Boston, MA, USA, and were executed according to the institutional guidelines.

For human analyses, 41 frozen colorectal cancer and paired normal colonic mucosa samples were provided by the tissue bank of the NCT Heidelberg and used according to the institutional guidelines of the tissue bank and according to the requirements of the ethics committee, University of Heidelberg, Germany.

Tumor analysis and tissue harvesting

For tumor quantification and measurements, freshly dissected colon samples were subjected to a microscopic screen.[10] *P*-values for comparison of Cre^- and Cre^+ were calculated using the two-tailed Mann–Whitney *U*-Test. Colon tumors were dissected and immediately frozen at −80 °C. Intestinal epithelial cells were harvested as described previously.[32] For microscopic analysis, freshly dissected colon was embedded in OCT or paraffin.

1lox/2lox genotyping

1lox/2lox genotyping of colonic mucosa and tumors was performed using competitive PCR and RealTime PCR as previously described.[10,11] To verify the competitive PCR, 1lox/2lox standards with different molar 1lox and 2lox ratios were prepared. For this purpose, 1lox- and 2lox-specific PCR products were generated using genomic DNA from $Dnmt3a^{(2lox/2lox)}$, $Fabpl^{4xat\text{-}132}\text{-}Cre^{(+/-)}$, $APC^{(Min/+)}$ transgenic mice and cloned into TA vectors (TOPO TA Cloning Kit for Sequencing, Life Technologies, Carlsbad, CA, USA). The concentration of 1lox and 2lox stock solution was measured using Nanodrop 1000 (Peqlab, Germany) and Quant-iT PicoGreen (Life Technologies).

Colonic microadenomas were identified and isolated as outlined in the study by Yamada *et al*.[33] (primary antibody for β-catenin staining: 610153, BD, Franklin Lakes, NJ, USA/1:500, pH 6; secondary antibody: Universal LSABTM2 Kit/HRP, DAKO, Glostrup, Denmark/1:200; HE counter stained). For 1lox/2lox allele genotyping, each microadenoma sample was subjected to three separate nested PCR reactions: 1lox-specific reaction, 2lox-specific reaction and reference PCR reaction upstream of the loxP sites. Primer sequences and reaction conditions are listed in Supplementary Table 4.

RNA FISH

RNA FISH probes for Dnmt3a transcript detection were placed in regions common to both Dnmt3a isoforms (NM_007872.4, NM_153743.3) with no homology to transcripts of Dnmt1, Dnmt2, Dnmt3b and Dnmt3L. The alignment program BLAST was used for sequence alignments (http://www.pubmed.com). RNA FISH analysis of Dnmt3a and Lgr5 expression was performed as described previously.[34,35] Probe sequences are listed in Supplementary Table 5. The error of the signal density was computed by bootstrap resampling of the image patches analyzed. *P*-values for the comparisons between different densities were calculated using the one-sided *t*-test with $\alpha = 0.05$.

Immunohistochemistry

For immunohistochemistry, a Dnmt3a antibody (ab14291, Abcam, Cambridge, UK[5,36,37]) recognizing amino acids 1–300 of the Dnmt3a isoform 1 (NP_031898.1) was used. Lack of homology of this region to Dnmt1, Dnmt2, Dnmt3b and Dnmt3L proteins was confirmed by sequence alignment using the alignment program BLAST (http://www.pubmed.com). Paraffin-embedded cross-sections of the mouse colon containing tumor tissue were cut into 1-µm thick sections. The sections were then stained with the Dnmt3a primary antibody at 1:40 dilution (pH 6) followed by staining with the secondary antibody at 1:200 dilution (ab6752, Abcam). Dnmt3a immunostaining of Cre^- colon mucosa was quantified using ImageJ-win64 (version 1.48s, National Institutes of Health, Bethesda, MD, USA, free download at: http://imagej.nih.go/ij/download/) image processing and analysis software (Supplementary Figure 3).

Microarray

For microarray analysis, the Illumina MouseWG-6v2.0 (Illumina, Hayward, CA, USA) platform was used according to the manufacturer's protocol. For microarray scanning, an iScan array scanner was used. For all beads, data

extraction was conducted individually. Outliers were removed when >2.5 median absolute deviation. The remaining data points were used for calculation of the mean average signal and the standard deviation for a given probe. Differential expression between Cre^+ and the Cre^- samples was defined as expression ratio $\geqslant 1.5$ and corrected (Benjamini-Hochberg) *P*-value < 0.05. IPA software was used for pathway analysis of differentially expressed genes (http://www.ingenuity.com). The data discussed in this publication have been deposited in NCBI's GEO (accession number: GSE48115, http://www.ncbi.nlm.nih.gov/geo/ query/acc.cgi?acc = GSE48115).

SYBR Green-based real-time PCR

DNAseI-treated RNA was converted to cDNA using the verso cDNA kit (Thermo Scientific, Waltham, MA, USA). Real-time PCR was performed using the LightCycler480 system (Roche Applied Science, Mannheim, Germany). Reaction efficiencies were measured using standard dilution curves. Each sample was measured in triplicates relative to a reference transcript (β-actin for Dnmt3a, GAPDH for Oct4, Tff2 and Cdkn1c). Data analysis occurred via Roche Applied Science software using the E-Method. Primer sequences and reaction conditions are listed in Supplementary Table 4.

Luminometric methylation assay

The Luminometric Methylation Assay was performed as described in the study by Karimi *et al*.[38] Briefly, ratios of *Msp*I restriction overhangs relative to *Hpa*II restriction overhangs (each corrected by reference *Eco*RI overhangs) were calculated using peak heights as measured by PSQ HS96A software (Biotage/Qiagen, Venlo, the Netherlands). A universal calibrator was used to enable normalization and quantitative comparison between different reaction plates.

454 Bisulfite sequencing

Genomic DNA (500 ng) was bisulfite treated according to the manufacturer's protocol (Imprint DNA Modification Kit, Sigma-Aldrich, St Louis, MO, USA). Regions of interest were amplified by (nested) PCR followed by PCR-based fusion of the 454 adapters to each gel extracted amplicon. Primer sequences and reaction conditions are listed in Supplementary Table 4. Tagged PCR products were gel purified and subjected to sequencing using the 454 platform (Roche Applied Science) according to the manufacturer's protocol.

Bioinformatical analyses

Expression of Dnmt3a in colon tumor and control tissue was evaluated using the available RNAseq data (41 controls, 258 tumor samples) from the cancer genome atlas (TCGA, URL: http://cancergenome.nih.gov). DNA methylation canyons were defined by using a two-state first-order Hidden Markov Model, as described previously[21] using published mouse colon methylation data[22] (GEO Accession-ID: GSM1051152) and a minimum length of 4.5 kb.

CONFLICT OF INTEREST

The authors declare no conflict of interest.

ACKNOWLEDGEMENTS

Support by the DKFZ Light Microscopy Facility is gratefully acknowledged. We also thank E Herpel and the tissue bank of the NCT Heidelberg for providing human tissue samples and for technical support in histology and immunohistochemistry. We also thank J Gutekunst for bioinformatical support and R Jaenisch for critical discussions. This study was supported by a graduate scholarship from the Helmholtz International Graduate School for Cancer Research (B Weis), a Burroughs-Wellcome Fund Career Award at the Scientific Interface (A Raj, H Maamar), a NIH Director's New Innovator award (1DP2OD008514–01 to A Raj) and the Lautenschläger foundation (HK Seitz).

REFERENCES

1 Jones PA, Baylin SB. The fundamental role of epigenetic events in cancer. *Nat Rev Genet* 2002; **3**: 415–428.
2 Okano M, Bell DW, Haber DA, Li E. DNA methyltransferases Dnmt3a and Dnmt3b are essential for de novo methylation and mammalian development. *Cell* 1999; **99**: 247–257.
3 Hsieh C-L. *In vivo* activity of murine de novo methyltransferases, Dnmt3a and Dnmt3b. *Mol Cell Biol.*, 1999; **19**: 8211–8218.
4 Samuel MS, Suzuki H, Buchert M, Putoczki TL, Tebbutt NC, Lundgren-May T *et al.* Elevated Dnmt3a activity promotes polyposis in Apc(Min) mice by relaxing extracellular restraints on Wnt signaling. *Gastroenterology* 2009; **137**: 902–913.
5 Linhart HG, Lin H, Yamada Y, Moran E, Steine EJ, Gokhale S *et al.* Dnmt3b promotes tumorigenesis in vivo by gene-specific de novo methylation and transcriptional silencing. *Genes Dev* 2007; **21**: 3110–3122.
6 Ley TJ, Ding L, Walter MJ, McLellan MD, Lamprecht T, Larson DE *et al.* DNMT3A mutations in acute myeloid leukemia. *New Engl J Med* 2010; **363**: 2424–2433.
7 Gao Q, Steine EJ, Barrasa MI, Hockemeyer D, Pawlak M, Fu D *et al.* Deletion of the de novo DNA methyltransferase Dnmt3a promotes lung tumor progression. *Proc Natl Acad Sci USA* 2011; **108**: 18061–18066.
8 Nguyen S, Meletis K, Fu D, Jhaveri S, Jaenisch R. Ablation of de novo DNA methyltransferase Dnmt3a in the nervous system leads to neuromuscular defects and shortened lifespan. *Dev Dyn* 2007; **236**: 1663–1676.
9 Saam JR, Gordon JI. Inducible gene knockouts in the small intestinal and colonic epithelium. *J Biol Chem* 1999; **274**: 38071–38082.
10 Lin H, Yamada Y, Nguyen S, Linhart H, Jackson-Grusby L, Meissner A *et al.* Suppression of Intestinal Neoplasia by Deletion of Dnmt3b. *Mol Cell Biol* 2006; **26**: 2976–2983.
11 Weis B, Schmidt J, Lyko F, Linhart H. Analysis of conditional gene deletion using probe based Real-Time PCR. *BMC Biotechnol* 2010; **10**: 75.
12 Yamada Y, Mori H. Multistep carcinogenesis of the colon in ApcMin/+ mouse. *Cancer Sci* 2007; **98**: 6–10.
13 Yang AS, Estecio MR, Doshi K, Kondo Y, Tajara EH, Issa JP. A simple method for estimating global DNA methylation using bisulfite PCR of repetitive DNA elements. *Nucleic Acids Res* 2004; **32**: e38.
14 Li JY, Pu MT, Hirasawa R, Li BZ, Huang YN, Zeng R *et al.* Synergistic function of DNA methyltransferases Dnmt3a and Dnmt3b in the methylation of Oct4 and Nanog. *Mol Cell Biol* 2007; **27**: 8748–8759.
15 Kaneda M, Okano M, Hata K, Sado T, Tsujimoto N, Li E *et al.* Essential role for de novo DNA methyltransferase Dnmt3a in paternal and maternal imprinting. *Nature* 2004; **429**: 900–903.
16 Peterson AJ, Menheniott TR, O'Connor L, Walduck AK, Fox JG, Kawakami K *et al. Helicobacter pylori* infection promotes methylation and silencing of Trefoil Factor 2, leading to gastric tumor development in mice and humans. *Gastroenterology* 2010; **139**: 2005–2017.
17 Katoh M. Trefoil factors and human gastric cancer (review). *Int J Mol Med* 2003; **12**: 3–9.
18 Kavanagh E, Joseph B. The hallmarks of CDKN1C (p57, KIP2) in cancer. *Biochimica et Biophysica Acta* 2011; **1816**: 50–56.
19 Matsuoka S, Edwards MC, Bai C, Parker S, Zhang P, Baldini A *et al.* p57KIP2, a structurally distinct member of the p21CIP1 Cdk inhibitor family, is a candidate tumor suppressor gene. *Genes Dev* 1995; **9**: 650–662.
20 Figliola R, Busanello A, Vaccarello G, Maione R. Regulation of p57KIP2 during muscle differentiation: role of Egr1, Sp1 and DNA hypomethylation. *J Mol Biol* 2008; **380**: 265–277.
21 Jeong M, Sun D, Luo M, Huang Y, Challen GA, Rodriguez B *et al.* Large conserved domains of low DNA methylation maintained by Dnmt3a. *Nat Genet* 2014; **46**: 17–23.
22 Hon GC, Rajagopal N, Shen Y, McCleary DF, Yue F, Dang MD *et al.* Epigenetic memory at embryonic enhancers identified in DNA methylation maps from adult mouse tissues. *Nat Genet* 2013; **45**: 1198–1206.
23 Jones PA, Baylin SB. The epigenomics of cancer. *Cell* 2007; **128**: 683–692.
24 Tang YA, Lin RK, Tsai YT, Hsu HS, Yang YC, Chen CY *et al.* MDM2 overexpression deregulates the transcriptional control of RB/E2F leading to DNA methyltransferase 3A overexpression in lung cancer. *Clin Cancer Res* 2012; **18**: 4325–4333.
25 He S, Wang F, Yang L, Guo C, Wan R, Ke A *et al.* Expression of DNMT1 and DNMT3a are regulated by GLI1 in human pancreatic cancer. *PLoS ONE* 2011; **6**: e27684.
26 Bai X, Song Z, Fu Y, Yu Z, Zhao L, Zhao H *et al.* Clinicopathological significance and prognostic value of DNA methyltransferase 1, 3a, and 3b expressions in sporadic epithelial ovarian cancer. *PLoS ONE* 2012; **7**: e40024.
27 Luczak MW, Roszak A, Pawlik P, Kedzia H, Kedzia W, Malkowska-Walczak B *et al.* Transcriptional analysis of CXCR4, DNMT3A, DNMT3B and DNMT1 gene expression in primary advanced uterine cervical carcinoma. *Int J Oncol* 2012; **40**: 860–866.
28 Rahman MM, Qian ZR, Wang EL, Yoshimoto K, Nakasono M, Sultana R *et al.* DNA methyltransferases 1, 3a, and 3b overexpression and clinical significance in gastroenteropancreatic neuroendocrine tumors. *Hum Pathol* 2010; **41**: 1069–1078.
29 Qu Y, Mu G, Wu Y, Dai X, Zhou F, Xu X *et al.* Overexpression of DNA methyltransferases 1, 3a, and 3b significantly correlates with retinoblastoma tumorigenesis. *Am J Clin Pathol* 2010; **134**: 826–834.

30 Hlady RA, Novakova S, Opavska J, Klinkebiel D, Peters SL, Bies J *et al.* Loss of Dnmt3b function upregulates the tumor modifier Ment and accelerates mouse lymphomagenesis. *J Clin Invest* 2012; **122**: 163–177.
31 Raddatz G, Gao Q, Bender S, Jaenisch R, Lyko F. Dnmt3a protects active chromosome domains against cancer-associated hypomethylation. *PLoS Genet* 2012; **8**: e1003146.
32 Fujimoto K, Beauchamp RD, Whitehead RH. Identification and isolation of candidate human colonic clonogenic cells based on cell surface integrin expression. *Gastroenterology* 2002; **123**: 1941–1948.
33 Yamada Y, Jackson-Grusby L, Linhart H, Meissner A, Eden A, Lin H *et al.* Opposing effects of DNA hypomethylation on intestinal and liver carcinogenesis. *Proc Natl Acad Sci USA* 2005; **102**: 13580–13585.
34 Steine EJ, Ehrich M, Bell GW, Raj A, Reddy S, van Oudenaarden A *et al.* Genes methylated by DNA methyltransferase 3b are similar in mouse intestine and human colon cancer. *J Clin Invest* 2011; **121**: 1748–1752.
35 Raj A, van den Bogaard P, Rifkin SA, van Oudenaarden A, Tyagi S. Imaging individual mRNA molecules using multiple singly labeled probes. *Nat Methods* 2008; **5**: 877–879.
36 Kinney SM, Chin HG, Vaisvila R, Bitinaite J, Zheng Y, Esteve PO *et al.* Tissue-specific distribution and dynamic changes of 5-hydroxymethylcytosine in mammalian genomes. *J Biol Chem* 2011; **286**: 24685–24693.
37 Morey Kinney SR, Smiraglia DJ, James SR, Moser MT, Foster BA, Karpf AR. Stage-specific alterations of DNA methyltransferase expression, DNA hypermethylation, and DNA hypomethylation during prostate cancer progression in the transgenic adenocarcinoma of mouse prostate model. *Mol Cancer Res* 2008; **6**: 1365–1374.
38 Karimi M, Johansson S, Stach D, Corcoran M, Grandér D, Schalling M *et al.* LUMA (LUminometric Methylation Assay)-A high throughput method to the analysis of genomic DNA methylation. *Exp Cell Res* 2006; **312**: 1989–1995.

Supplementary Information accompanies this paper on the Oncogene website (http://www.nature.com/onc)